

Wavelength dependence of crosstalk in dual-wavelength measurement of oxy- and deoxy-hemoglobin

Nobuhiro Okui
Eiji Okada

Keio University
Department of Electronics and Electrical Engineering
3-14-1, Hiyoshi, Kohoku-ku
Yokohama, 223-8522, JAPAN
E-mail: nobu@okd.elec.keio.ac.jp

Abstract. In near-IR spectroscopy, the concentration change in oxy- and deoxyhemoglobin in tissue is calculated from the change in the detected intensity of light at two wavelengths by solving the simultaneous equation based on the modified Lambert-Beer law. The wavelength-independent constant or mean optical path length is usually assigned to the term of partial optical path length in the simultaneous equation. This insufficient optical path length in the calculation causes crosstalk between the concentration change in oxy- and deoxyhemoglobin. We investigate the crosstalk in the dual-wavelength measurement of oxy- and deoxyhemoglobin theoretically by Monte Carlo simulation to discuss the optimal wavelength pair to minimize the crosstalk. The longer wavelength of the dual-wavelength measurement is fixed at 830 nm and the shorter wavelength is varied from 650 to 780 nm. The optimal wavelength range for pairing with 830 nm for the dual-wavelength measurement of oxy- and deoxyhemoglobin is from 690 to 750 nm. The mean optical path length, which can be obtained by time- and phase-resolved measurement, is effective to reduce the crosstalk in the results of dual-wavelength measurement.

© 2005 Society of Photo-Optical Instrumentation Engineers. [DOI: 10.1117/1.1846076]

Keywords: near-infrared spectroscopy; crosstalk; wavelength pair; Monte Carlo simulation.

Paper NEU-03 received Feb. 5, 2004; revised manuscript received May 1, 2004; accepted for publication May 17, 2004; published online Jan. 31, 2005.

1 Introduction

Near-IR spectroscopy (NIRS), which can obtain the concentration change in oxy- and deoxyhemoglobin in tissue from the change in detected intensity of near-IR light, has been applied to noninvasively measure human brain activation.¹⁻³ The concentration change in oxy- and deoxyhemoglobin can be independently calculated from the change in the intensity of the detected light at two wavelengths, the molar extinction coefficients of oxy- and deoxyhemoglobin, and the partial optical path length that the detected light travels in the activated region by solving the simultaneous equation based on the modified Lambert-Beer law⁴ (MLBL). Theoretical modeling of light propagation in the head is essential to estimate the partial optical path length because it is impossible to directly measure the partial optical path length by experiments. It is rather difficult to consider sophisticated anatomical configuration and optical properties of tissue in the head to estimate accurate partial optical path length. The theoretical estimation for individual subjects is rarely performed in practical measurements. Alternatively, the wavelength-independent constant is normally assigned to the term of partial optical path length in the simultaneous equation for MLBL calculation in a

cw NIRS instrument. Time- and phase-resolved instrument can measure the mean optical path length that the detected light travels in a whole head.^{5,6} The wavelength-dependent mean optical path length is frequently assigned to the MLBL calculation to obtain the concentration change in oxy- and deoxyhemoglobin. It is revealed that this insufficient optical path length in the MLBL calculation causes the crosstalk between the concentration changes in oxy- and deoxyhemoglobin in the result of NIRS measurement.^{7,8} The crosstalk depends on the selection of wavelength pair for NIRS measurement because the crosstalk is caused by the difference between the actual partial optical path length and the path length in the MLBL calculation. However, the optimal wavelength selection of the dual-wavelength measurement based on the MLBL calculation from the viewpoint of minimizing the crosstalk has not yet been investigated.

In this paper, we theoretically investigated the crosstalk from oxy- to deoxyhemoglobin and from deoxy- to oxyhemoglobin in the dual-wavelength measurement of brain activity based on the MLBL calculation with cw and time-resolved NIRS instruments. The change in intensity of the detected light at seven wavelengths from 650 to 830 nm caused by the change in either oxy- or deoxyhemoglobin in the gray matter in the adult head model was predicted by Monte Carlo simu-

Address all correspondence to Nobuhiro Okui, 3-14-1, Hiyoshi, Kohoku-ku, Yokohama, 223-8522 Japan. Tel: +81-(0)-45-566-1532; Fax: +81-(0)-45-566-1529; E-mail: nobu@okd.elec.keio.ac.jp

lation. The change in intensity for the head model including skull and cerebrospinal fluid (CSF) layers of various thicknesses was obtained to investigate the influence of thickness of the superficial tissues on crosstalk. The crosstalk was deduced from the results of concentration change of oxy- and deoxyhemoglobin calculated from the change in the detected intensity by dual-wavelength measurement using the MLBL. The longer wavelength of the dual-wavelength measurement was fixed at 830 nm and the shorter wavelength was varied from 650 to 780 nm to evaluate the optimal wavelength pair to minimize crosstalk. In the MLBL calculation, the wavelength-independent constant and the wavelength-dependent mean optical path length were assigned to the terms of wavelength-dependent partial optical path length to discuss the effect of time- and phase-resolved measurement on the crosstalk. The change in intensity for the head model including skull and CSF layers of various thicknesses was obtained to investigate the influence of thickness of the superficial tissues on the crosstalk.

2 NIRS and Crosstalk

Brain activation causes the change in concentration of oxy- and deoxyhemoglobin in cortical tissue. In NIRS measurement, the intensity change of the detected light is measured and the relationship between the change in measured optical density ΔOD and the change in concentration of oxyhemoglobin Δc_{oxy} and deoxyhemoglobin Δc_{deoxy} is described by a Lambert-Beer law:¹

$$\Delta OD(\lambda) = [\Delta c_{\text{oxy}} \epsilon_{\text{oxy}}(\lambda) + \Delta c_{\text{deoxy}} \epsilon_{\text{deoxy}}(\lambda)] \langle L(\lambda) \rangle, \quad (1)$$

where ϵ_{oxy} and ϵ_{deoxy} are the molar extinction coefficients of oxy- and deoxyhemoglobin, and $\langle L \rangle$ is the mean optical path length of the detected light. The mean optical path length is considerably longer than the geometric distance between the source and the detector because the detected light is scattered in biological tissue. Although Eq. (1) is assumed that the concentration of oxy- and deoxyhemoglobin is homogeneously changed in the whole volume of tissue where the detected light passes, the concentration of oxy- and deoxyhemoglobin is locally changed during brain activation. Assuming that oxy- and deoxyhemoglobin is changed only in the cortex during brain activation, the change in intensity detected with NIRS instrument is given by

$$\Delta OD(\lambda) = [\Delta c_{\text{oxy}} \epsilon_{\text{oxy}}(\lambda) + \Delta c_{\text{deoxy}} \epsilon_{\text{deoxy}}(\lambda)] \langle L_{\text{cortex}}(\lambda) \rangle, \quad (2)$$

where $\langle L_{\text{cortex}}(\lambda) \rangle$ is the partial optical path length in the cortical tissue, which is considerably shorter than the mean optical path length. The change in the concentration of oxy- and deoxyhemoglobin can be individually calculated from the change in intensity of the detected light at two wavelengths by solving simultaneous equation derived from Eq. (2).

$$\Delta c_{\text{oxy}}^*(\lambda_1, \lambda_2) = \frac{\Delta OD(\lambda_2) \epsilon_{\text{deoxy}}(\lambda_1) \langle L_{\text{cortex}}(\lambda_1) \rangle - \Delta OD(\lambda_1) \epsilon_{\text{deoxy}}(\lambda_2) \langle L_{\text{cortex}}(\lambda_2) \rangle}{[\epsilon_{\text{oxy}}(\lambda_1) \epsilon_{\text{deoxy}}(\lambda_2) - \epsilon_{\text{oxy}}(\lambda_2) \epsilon_{\text{deoxy}}(\lambda_1)] \langle L_{\text{cortex}}(\lambda_1) \rangle \langle L_{\text{cortex}}(\lambda_2) \rangle} \quad (3a)$$

$$\Delta c_{\text{deoxy}}^*(\lambda_1, \lambda_2) = \frac{\Delta OD(\lambda_1) \epsilon_{\text{oxy}}(\lambda_2) \langle L_{\text{cortex}}(\lambda_2) \rangle - \Delta OD(\lambda_2) \epsilon_{\text{oxy}}(\lambda_1) \langle L_{\text{cortex}}(\lambda_1) \rangle}{[\epsilon_{\text{oxy}}(\lambda_1) \epsilon_{\text{deoxy}}(\lambda_2) - \epsilon_{\text{oxy}}(\lambda_2) \epsilon_{\text{deoxy}}(\lambda_1)] \langle L_{\text{cortex}}(\lambda_1) \rangle \langle L_{\text{cortex}}(\lambda_2) \rangle} \quad (3b)$$

where $\Delta c_{\text{oxy}}^*(\lambda_1, \lambda_2)$ and $\Delta c_{\text{deoxy}}^*(\lambda_1, \lambda_2)$ are the measured concentration change in oxy- and deoxyhemoglobin calculated from the change in the intensity of the detected light at wavelengths λ_1 and λ_2 . Equations (3a) and (3b) show that the partial optical path length in the cortical tissue is necessary to calculate the concentration change in oxy- and deoxyhemoglobin. However, the partial optical path length in the cortical tissue can not be directly measured by experiments. In practical measurement by MLBL calculation, wavelength-independent constant or wavelength-dependent mean optical path length is assigned to the term of the partial optical path length in Eqs. (3a) and (3b) for the calculation of the concentration change. This imprecise path length in the simultaneous equation leads to error in the measured concentration change and this insufficient separation of the change in oxy- and deoxyhemoglobin is called crosstalk. The crosstalk is defined that the ratio of the measured concentration change of chromophore for which no change was induced and the measured concentration change of another chromophore for which the change was induced.⁷ The crosstalk from the con-

centration change of oxyhemoglobin to concentration change of deoxyhemoglobin $c_{\text{oxy} \rightarrow \text{deoxy}}(\lambda)$ and that from deoxyhemoglobin to oxyhemoglobin $c_{\text{deoxy} \rightarrow \text{oxy}}(\lambda)$ can be given as follows:

$$C_{\text{oxy} \rightarrow \text{deoxy}}(\lambda_1, \lambda_2) = \Delta c_{\text{deoxy}}^*(\lambda_1, \lambda_2) / \Delta c_{\text{oxy}}^*(\lambda_1, \lambda_2), \quad (4a)$$

$$C_{\text{deoxy} \rightarrow \text{oxy}}(\lambda_1, \lambda_2) = \Delta c_{\text{oxy}}^*(\lambda_1, \lambda_2) / \Delta c_{\text{deoxy}}^*(\lambda_1, \lambda_2). \quad (4b)$$

The crosstalk is proportional to the difference in the relative path length at two wavelengths.⁷ The relative path length is the ratio between the actual partial optical path length and the path length using in the MLBL calculation. If the partial optical path length at two wavelengths is the same [$\langle L_{\text{cortex}}(\lambda_1) \rangle = \langle L_{\text{cortex}}(\lambda_2) \rangle$], the crosstalk can be easily canceled. One of the best ways to minimize the crosstalk is to choose the wavelength pair at which the partial optical path length in the cortical tissue is the same.

Table 1 The wavelength-dependent optical properties (absorption coefficient μ_a and transport scattering coefficient μ'_s) and thickness of each layer of the head model.

Wavelength (nm)	650		670		690		720	
	μ_a (mm ⁻¹)	μ'_s (mm ⁻¹)	μ_a	μ'_s	μ_a	μ'_s	μ_a	μ'_s
Scalp	0.037	2.62	0.031	2.53	0.026	2.38	0.022	2.24
Skull	0.033	2.54	0.027	2.33	0.017	2.13	0.013	1.92
CSF	0.0053	0.38	0.0044	0.35	0.0029	0.32	0.003	0.29
Gray matter	0.058	2.77	0.048	2.69	0.039	2.57	0.036	2.46
White matter	0.030	10.95	0.024	10.49	0.018	10.03	0.014	9.78
Wavelength (nm)	750		780		830		Thickness (mm)	
	μ_a	μ'_s	μ_a	μ'_s	μ_a	μ'_s		
Scalp	0.022	2.11	0.020	2.00	0.019	1.84	3	
Skull	0.016	1.79	0.016	1.66	0.017	1.47	4,7,12 (CSF:2)	
CSF	0.0045	0.27	0.0044	0.25	0.0056	0.22	0.5,1,5 (skull:7)	
Gray matter	0.038	2.39	0.036	2.31	0.041	2.10	4	
White matter	0.016	9.62	0.016	9.25	0.018	8.82	20	

3 Simulation Method

The adult head model for simulation to investigate the crosstalk is a five-layered slab that consists of the scalp, skull, CSF layer, gray matter, and white matter. The propagation of light at seven wavelengths, 650, 670, 690, 720, 750, 780, and 830 nm, was predicted to evaluate the crosstalk in dual-wavelength measurement of oxy- and deoxyhemoglobin. The wavelength-dependent optical properties (absorption coefficient μ_a and transport scattering coefficient μ'_s) and thickness of each layer of the head model are shown in Table 1. They were chosen from reported data for dermis,⁹ pig skull,¹⁰ and human brain¹¹ measured with an integrating sphere system. The optical properties of the CSF layer were estimates based on the previous results.¹² The thickness of the skull was altered from 4 to 12 mm with the CSF thickness held constant at 2 mm. Similarly, the CSF layer thickness was altered from 0.5 to 5 mm with the skull thickness held constant at 7 mm.

The light propagation in the head model was predicted by Monte Carlo simulation to obtain the mean optical path length and the partial optical path length in the gray matter for the source-detector spacing of 30 and 40 mm. The detail algorithm of Monte Carlo simulation is described elsewhere.^{13,14} The change in the intensity of the detected light at each wavelength $\Delta OD(\lambda)$ induced by either oxy- or deoxyhemoglobin was calculated as follows:

$$\Delta OD_{oxy}(\lambda) = [\Delta c_{oxy} \epsilon_{oxy}(\lambda)] \langle L_{graymatter}(\lambda) \rangle, \quad (5a)$$

$$\Delta OD_{deoxy}(\lambda) = [\Delta c_{deoxy} \epsilon_{deoxy}(\lambda)] \langle L_{graymatter}(\lambda) \rangle, \quad (5b)$$

where $\langle L_{graymatter}(\lambda) \rangle$ is the partial optical path length in the gray matter of the model. The concentration change of oxy- and deoxyhemoglobin in the gray matter is assumed to be 10 μM . The measured concentration change of oxyhemoglobin Δc_{oxy}^* and deoxyhemoglobin Δc_{deoxy}^* obtained by the NIRS instruments was calculated from the detected intensity at two wavelength by the MBL calculation. The longer wavelength λ_2 of the dual-wavelength measurement was fixed at 830 nm and the shorter wavelength λ_1 was varied to be 650, 670, 690, 720, 750, and 780 nm. Either wavelength-independent constant or the mean optical path length was assigned to the terms of the partial optical path length in Eqs. (3a) and (3b) because the partial optical path length cannot be directly obtained by experiment. We used $\langle L_{cortex}(\lambda_1) \rangle = \langle L_{cortex}(\lambda_2) \rangle = 1$ for wavelength-independent constant. This assignment is often applied to near-IR topography.¹⁵ The crosstalk from oxy- to deoxyhemoglobin $C_{oxy \rightarrow deoxy}$ and from deoxy- to oxyhemoglobin $C_{deoxy \rightarrow oxy}$ for each wavelength pair was calculated from the measured concentration change of oxyhemoglobin and deoxyhemoglobin by Eqs. (4a) and (4b).

4 Results

4.1 Wavelength Dependence of Partial Optical Path Length

Figures 1 and 2 show the wavelength dependence of the partial optical path length in the gray matter predicted by Monte Carlo simulation. Two peaks at about 720 and 780 nm can be observed in all the results. The two peaks are related to the absorption properties of tissue, especially to the absorption spectrum of oxyhemoglobin because the light that travels a

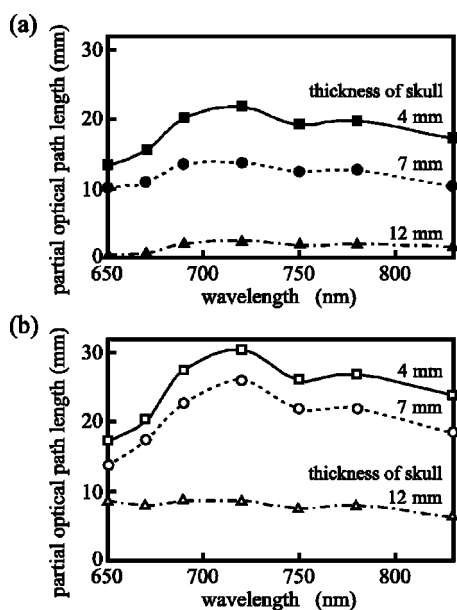


Fig. 1 Effect of the skull thickness on the wavelength dependence of the partial optical path length in the gray matter for source-detector spacings of (a) 30 and (b) 40 mm. The partial optical path length at seven wavelengths predicted by Monte Carlo simulation was interpolated to obtain the curve.

long path length is highly attenuated in tissues with a high absorption coefficient. The effect of the skull thickness on the partial optical path length for source-detector spacing of 30 and 40 mm is shown in Figs. 1(a) and 1(b), respectively. The partial optical path length in the gray matter decreases with an increase in skull thickness. The light takes a longer path

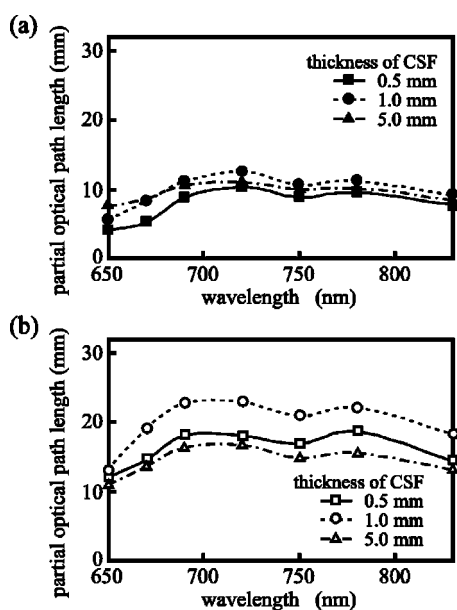


Fig. 2 Effect of the CSF thickness on the wavelength dependence of the partial optical path length in the gray matter for source-detector spacings of (a) 30 and (b) 40 mm. The partial optical path length at seven wavelengths predicted by Monte Carlo simulation was interpolated to obtain the curve.

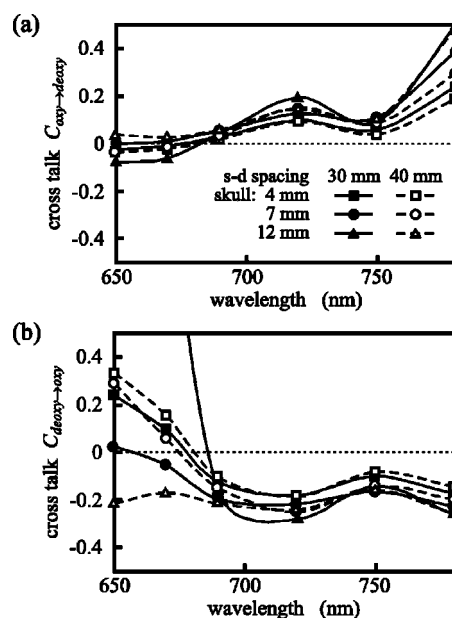


Fig. 3 Effect of skull thickness on the crosstalk (a) from oxy- to deoxyhemoglobin $C_{oxy \rightarrow deoxy}$ and (b) from deoxy- to oxyhemoglobin $C_{deoxy \rightarrow oxy}$. The wavelength-independent constant is used for MLBL calculation. The skull thickness is varied from 4 to 12 mm.

length to reach a deeper region, and hence the attenuation of light traveling in deep gray matter is greater than that traveling in shallow gray matter. The two peaks are significantly observed when the skull thickness is thin and the source-detector spacing is large. In the case where the source-detector spacing is 30 mm, the wavelength at which the partial optical path length is the same as that at 830 nm for the model with skull layer of 4-, 7-, and 12-mm thickness is about 670, 650, and 690 nm, respectively. The effect of the CSF thickness on the partial optical path length for source-detector spacings of 30 and 40 mm is shown in Figs. 2(a) and 2(b), respectively. The partial optical path length is not proportionally increased with an increase in CSF thickness. The partial optical path length for the model with a CSF layer of 1-mm thickness is greater than that for the models with CSF layers of 0.5- and 5.0-mm thicknesses. The wavelength dependence of the partial optical path length is almost the same for all the models with various thicknesses of the CSF. The effect of the CSF thickness on the partial optical path length is less than that of the skull thickness. The difference in the effect of thickness between the skull and CSF layer is caused by the difference in their optical properties. Both the scattering and absorption coefficients of the CSF layer are much smaller than those of the skull. The wavelength at which the partial optical path length is the same as that at 830 nm is also varied with the CSF thickness.

4.2 Crosstalk in MLBL Calculation with Wavelength-Independent Path Length

The crosstalk from oxy- to deoxyhemoglobin $C_{oxy \rightarrow deoxy}$ and from deoxy- to oxyhemoglobin $C_{deoxy \rightarrow oxy}$ as a function of shorter wavelength is shown in Figs. 3(a) and 3(b), respectively. The crosstalk was calculated from the measured concentration change of oxyhemoglobin and deoxyhemoglobin

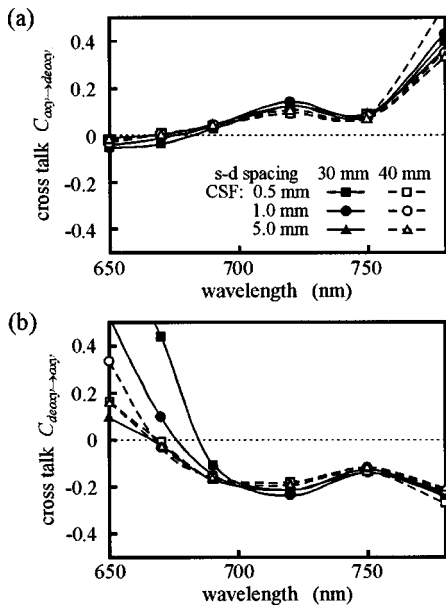


Fig. 4 Effect of CSF thickness on the crosstalk (a) from oxy- to deoxyhemoglobin $C_{oxy \rightarrow deoxy}$ and (b) from deoxy- to oxyhemoglobin $C_{deoxy \rightarrow oxy}$. The wavelength-independent constant is used for MLBL calculation. The CSF thickness is varied from 0.5 to 5 mm.

calculated with the wavelength-independent constant path length ($\langle L_{cortex}(\lambda_1) \rangle = \langle L_{cortex}(\lambda_2) \rangle = 1$). The thickness of the skull was varied from 4 to 12 mm. The crosstalk from oxy- to deoxyhemoglobin $C_{oxy \rightarrow deoxy}$ is very small when the shorter wavelength is shorter than 690 nm. The measured change in concentration of deoxyhemoglobin tends to be overestimated by the influence of the crosstalk in the case where the shorter wavelength is longer than 690 nm. The crosstalk steeply increases when the shorter wavelength is beyond 750 nm. The wavelength dependence of the crosstalk from deoxy- to oxyhemoglobin $C_{deoxy \rightarrow oxy}$ is entirely different from that from oxy- to deoxyhemoglobin $C_{oxy \rightarrow deoxy}$. The crosstalk is almost constant and the measured change in concentration of oxyhemoglobin is underestimated by the influence of the crosstalk when the shorter wavelength is longer than 690 nm. The crosstalk steeply varies with wavelength in the case where the shorter wavelength is shorter than 690 nm. The measured change in concentration of oxyhemoglobin tends to be overestimated when the shorter wavelength is shorter than 670 nm, barring few exceptions. The influence of the crosstalk both from oxy- to deoxyhemoglobin and deoxy- to oxyhemoglobin slightly increases with a increase in the skull thickness. The effect of the CSF thickness on the wavelength dependence of the crosstalk from oxy- to deoxyhemoglobin $C_{oxy \rightarrow deoxy}$ and from deoxy- to oxyhemoglobin $C_{deoxy \rightarrow oxy}$ is shown in Figs. 4(a) and 4(b), respectively. The wavelength dependence of the crosstalk both from oxy- to deoxyhemoglobin $C_{oxy \rightarrow deoxy}$ and from deoxy- to oxyhemoglobin $C_{deoxy \rightarrow oxy}$ is the same as those shown in Figs. 3(a) and 3(b). The effect of the difference in the CSF thickness is significant only in crosstalk from deoxy- to oxyhemoglobin $C_{deoxy \rightarrow oxy}$ when the shorter wavelength is less than 690 nm.

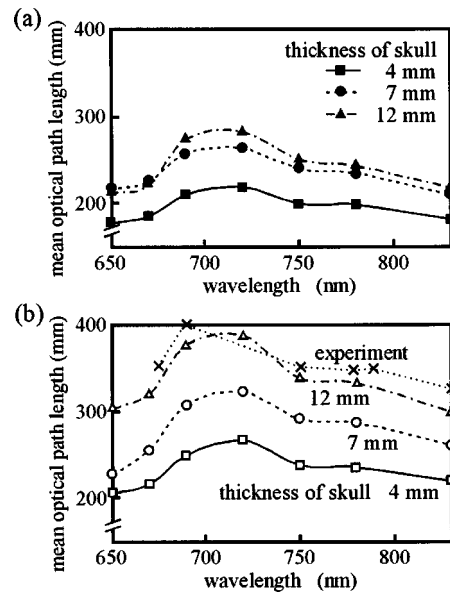


Fig. 5 Effect of the skull thickness on the wavelength dependence of the mean optical path length for source-detector spacings of (a) 30 and (b) 40 mm. The mean optical path length at seven wavelengths predicted by Monte Carlo simulation was interpolated to obtain the curve. The experimental data in (b) were calculated from differential pathlength factor reported by Stangman et al.⁸

4.3 Crosstalk in MLBL Calculation with Mean Optical Path Length

Figures 5 and 6 show the wavelength dependence of the mean optical path length predicted by Monte Carlo simulation. A peak at about 710 nm can be remarkably observed in all the results. Another peak at about 770 nm can also be observed in

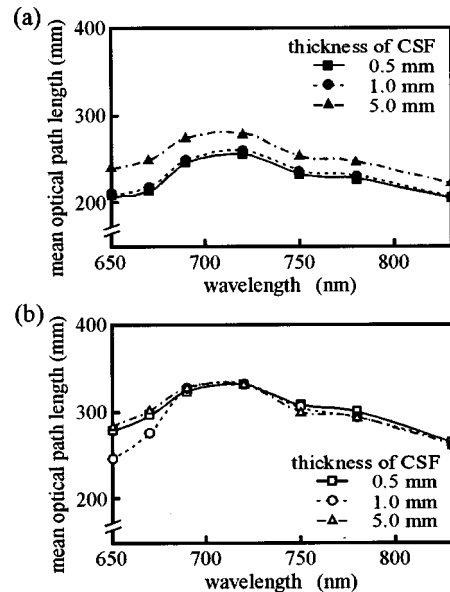


Fig. 6 Effect of the CSF thickness on the wavelength dependence of the mean optical path length for source-detector spacings of (a) 30 and (b) 40 mm. The mean optical path length at seven wavelengths predicted by Monte Carlo simulation was interpolated to obtain the curve.

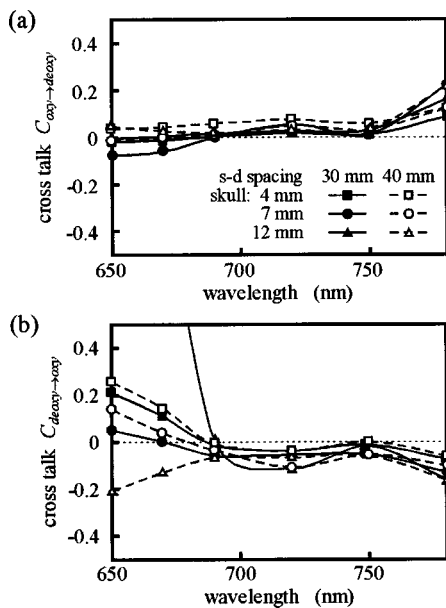


Fig. 7 Effect of skull thickness on the crosstalk (a) from oxy- to deoxyhemoglobin $C_{\text{oxy} \rightarrow \text{deoxy}}$ and (b) from deoxy- to oxyhemoglobin $C_{\text{deoxy} \rightarrow \text{oxy}}$. The wavelength-dependent mean optical path length is used for MLBL calculation. The skull thickness is varied from 4 to 12 mm.

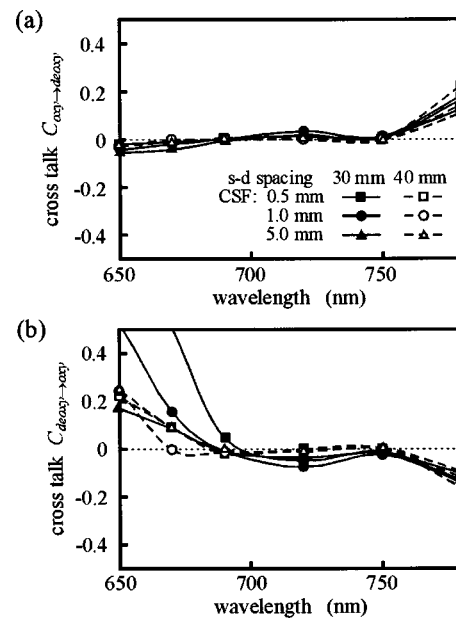


Fig. 8 Effect of CSF thickness on the crosstalk (a) from oxy- to deoxyhemoglobin $C_{\text{oxy} \rightarrow \text{deoxy}}$ and (b) from deoxy- to oxyhemoglobin $C_{\text{deoxy} \rightarrow \text{oxy}}$. The wavelength-dependent mean optical path length is used for MLBL calculation. The CSF thickness is varied from 0.5 to 5 mm.

some results. The experimental results in Fig. 5(b) are obtained from the figures that have experimentally derived values for differential pathlength factors of an adult head at 675-, 691-, 752-, 780-, 788-, and 830-nm wavelengths reported by Strangman et al.⁸ They measured the differential pathlength factor by the frequency-domain multidistance method with two sources located at 36 and 48 mm from a detector. The wavelength dependence of mean optical path length for the head model agrees well with the experimental results. The tendency of the wavelength dependence of the mean optical path length is similar to that of the partial optical path length shown in Figs. 1 and 2. The effect of the skull thickness on the mean optical path length for source-detector spacings of 30 and 40 mm is shown in Figs. 5(a) and 5(b), respectively. The mean optical path length increases with an increase in the skull thickness, whereas the partial optical path length decreases with an increase in the skull thickness. The influence of the CSF thickness on the mean optical path length shown in Fig. 6 is different from that on the partial optical path length shown in Fig. 2.

The mean optical path length depends on wavelength, thickness of the superficial tissues, and source-detector spacing. In the wavelength-dependent case, we assumed simultaneous measurement of the optical density and the mean optical path length by time- or phase-resolved instrumentation. The mean optical path length which is assigned to the term of the partial optical path length in Eqs. (3a) and (3b) for calculating the crosstalk is varied with the wavelength and thickness of the superficial tissues. The influence of the skull and CSF thickness on the crosstalk is shown in Figs. 7 and 8, respectively. The wavelength dependence of the crosstalk from oxy- to deoxyhemoglobin $C_{\text{oxy} \rightarrow \text{deoxy}}$ is shown in Figs. 7(a) and 8(a) and that from deoxy- to oxyhemoglobin

$C_{\text{deoxy} \rightarrow \text{oxy}}$ is shown in Figs. 7(b) and 8(b), respectively. The crosstalk from oxy- to deoxyhemoglobin $C_{\text{oxy} \rightarrow \text{deoxy}}$ slightly increases with an increase in wavelength when the shorter wavelength is longer than 750 nm. The measured deoxyhemoglobin tends to be barely overestimated in the other wavelength range. The crosstalk from deoxy- to oxyhemoglobin $C_{\text{deoxy} \rightarrow \text{oxy}}$ steeply varies with wavelength in the case where the shorter wavelength is shorter than 690 nm. The measured oxyhemoglobin is underestimated by the influence of the crosstalk in the other wavelength range. The crosstalk both from oxy- to deoxyhemoglobin $C_{\text{oxy} \rightarrow \text{deoxy}}$ and from deoxy- to oxyhemoglobin $C_{\text{deoxy} \rightarrow \text{oxy}}$ obtained by the MLBL calculation with the mean optical path length is remarkably smaller than that obtained by the MLBL calculation with the wavelength-independent path length.

5 Discussion

The crosstalk in dual-wavelength measurement is caused by the difference between the actual partial optical path length in the cortical tissue and the assumed path length in MLBL calculation. In the dual-wavelength measurement, sensitive measurement of the concentration of oxy- and deoxyhemoglobin occurs when the changes in the detected intensity are measured at wavelengths that straddle an isosbestic wavelength of hemoglobin. The small difference between the dual wavelengths seems to minimize the influence of scattering because scattering coefficient of the cortical tissue gradually decreases with increasing wavelength. These are the reason why the 780-/830-nm wavelength pair has been preferably used for the NIRS measurements. Uludag et al.⁷ revealed that the crosstalk is proportional to the difference in the relative partial path length, which is the ratio of the actual partial path length to the path length in MLBL calculation at two wavelengths. The

best way to minimize the crosstalk is to choose the wavelength pair at which the relative partial optical path length in the cortical tissue is the same. However, this minimization is not practical because the wavelength at which the partial optical path length is the same as that at 830 nm depends on the thickness of the skull and the CSF, as shown in Figs. 1 and 2. With respect to minimizing the difference in the relative partial path length, the 780-/830-nm wavelength pair seems a good choice. However, the crosstalk depends not only on the relative partial path length but also on the extinction coefficients of oxy- and deoxyhemoglobin. Strangman et al.⁸ investigated the contribution of the extinction coefficients of oxy- and deoxyhemoglobin to the wavelength dependence of the crosstalk. Although they did not consider the wavelength dependence of the partial optical path length, they showed the crosstalk grew quickly with wavelengths greater than approximately 770 nm when paired with 830 nm. As shown in Figs. 3 to 8, the crosstalk from oxy- to deoxyhemoglobin $C_{\text{oxy} \rightarrow \text{deoxy}}$ increases when the shorter wavelength is longer than 750 nm, and that from deoxy- to oxyhemoglobin $C_{\text{deoxy} \rightarrow \text{oxy}}$ increases when the shorter wavelength is less than 690 nm. Koizumi et al.¹⁵ evaluated the optimal wavelength pair from the point of view of the SNR of the detected signal. They concluded that 692-/830-nm wavelength pair produced a better SNR than the 782-/830-nm wavelength pair. These results suggested that the optimal wavelength range for pairing with 830 nm for the dual-wavelength measurement of oxy- and deoxyhemoglobin is from 690 to 750 nm.

The wavelength dependence of the mean optical path length is similar to that of the partial optical path length and the MLBL calculation with the mean optical path length significantly reduces the crosstalk, especially at the wavelength range from 690 to 750 nm. The mean optical path length can be experimentally measured by time- or phase-resolved instrumentation, whereas the partial optical path length cannot be directly measured by experiments. Note, however, that the effect of the skull and CSF thickness on the increase in the mean optical path length is different from that on the partial optical path length. The MLBL calculation with the mean optical path length is not effective to compensate for the difference in sensitivity caused by the thickness variation of the skull and CSF.

6 Conclusions

The crosstalk in the dual-wavelength measurement of oxy- and deoxyhemoglobin based on the MLBL calculation with cw and time-resolved NIRS instruments was theoretically investigated by Monte Carlo simulation. The light propagation in the adult head model including skull and CSF layers of various thicknesses was predicted to obtain the change in the detected intensity of light at seven wavelengths, the partial optical path length in the gray matter and the mean optical path length. The crosstalk in the MLBL calculations with the wavelength-independent path length and the wavelength-dependent mean optical path length was calculated for various wavelength pairs. The longer wavelength of the dual-wavelength measurement was fixed at 830 nm and the shorter wavelength was varied from 650 to 780 nm to evaluate the optimal wavelength pair to minimize the crosstalk.

The wavelength dependence of the crosstalk was varied with the skull and CSF thickness. Although the best way to minimize the crosstalk is to choose the wavelength pair at which the partial optical path length in the cortical tissue is the same, the optimal wavelength pair depends on the thickness of the superficial tissues. It is difficult to give a general optimal wavelength pair to minimize the crosstalk. The crosstalk from oxy- to deoxyhemoglobin increases when the shorter wavelength is longer than 750 nm, and that from deoxy- to oxyhemoglobin increases when the shorter wavelength is less than 690 nm. The crosstalk from oxy- to deoxyhemoglobin and that from deoxy- to oxyhemoglobin cannot be minimized for the same wavelengths. These results indicate that the wavelength range from 690 to 750 nm is a good trade-off for pairing with 830 nm for the dual-wavelength measurement of oxy- and deoxyhemoglobin to minimize crosstalk in both cases. The mean optical path length, which can be obtained by time- and phase-resolved measurement, is effective to reduce the crosstalk in the results of MLBL calculation. A theoretical prediction of partial optical path length in head model with adequate anatomical segmentation and optical properties will be effective for not only quantitative measurement but also to minimize the crosstalk.

Acknowledgments

This research was partly supported by Japan Society for the Promotion of Science, Grants-in-Aid for Scientific Research No. 13558116, and Grant-in-Aid for the 21st Century Center of Excellence for Optical and Electronic Device Technology for Access Network from the Ministry of Education, Culture, Sport, Science and Technology in Japan.

References

1. B. C. Wilson, E. M. Sevick, M. S. Patterson, and B. Chance, "Time-dependent optical spectroscopy and imaging for biomedical applications," *Proc. IEEE* **80**, 918–930 (1992).
2. Y. Hoshi and M. Tamura, "Detection of dynamic changes in cerebral oxygenation coupled to neural function during mental work in man," *J. Neurosci.* **150**, 5–8 (1993).
3. M. Ferrari, R. A. De Blasi, S. Fantini, M. A. Franceschini, B. Barbieri, V. Quaresima, and E. Gratton, "Cerebral and muscle oxygen saturation measurement by frequency-domain near-infrared spectroscopic technique," *Proc. SPIE* **2389**, 868–874 (1995).
4. S. J. Matcher, C. E. Elwell, C. E. Cooper, M. Cope, and D. T. Delpy, "Performance comparison of several published tissue near-infrared spectroscopy algorithms," *Anal. Biochem.* **227**, 54–68 (1995).
5. M. Oda, Y. Yamashita, T. Nakano, A. Suzuki, K. Shimizu, I. Hirano, F. Shimomura, E. Ohmae, T. Suzuki, and Y. Tsuchiya, "Near-infrared time-resolved spectroscopy system for tissue oxygenation monitor," *Proc. SPIE* **3597**, 611–617 (1999).
6. H. Y. Ma, Q. Xu, J. R. Ballesteros, V. Ntziachristos, Q. Zhang, and B. Chance, "Quantitative study of hypoxia stress in piglet brain by IQ phase modulation oximetry," *Proc. SPIE* **3597**, 642–649 (1999).
7. K. Uludag, M. Kohl, J. Steinbrink, H. Obrig, and A. Villringer, "Cross talk in the Lambert-Beer calculation for near-infrared wavelengths estimated by Monte Carlo simulations," *J. Biomed. Opt.* **7**, 51–59 (2002).
8. G. Strangman, M. A. Franceschini, and D. A. Boas, "Factors affecting the accuracy of near-infrared spectroscopy concentration calculations for focal changes in oxygenation parameters," *Neuroimage* **18**, 865–879 (2003).
9. C. R. Simpson, M. Kohl, M. Essenpreis, and M. Cope, "Near-infrared optical properties of ex vivo human skin and subcutaneous tissues measured using the Monte Carlo inversion technique," *Phys. Med. Biol.* **43**, 2465–2478 (1998).

10. M. Firbank, M. Hiraoka, M. Essenpreis, and D. T. Delpy, "Measurement of the optical properties of the skull in the wavelength range 650–950 nm," *Phys. Med. Biol.* **38**, 503–510 (1993).
11. P. van der Zee, M. Essenpreis, and D. T. Delpy, "Optical properties of brain tissue," *Proc. SPIE* **1888**, 454–465 (1993).
12. E. Okada and D. T. Delpy, "Near-infrared light propagation in an adult head model. I. Modeling of low-level scattering in the cerebrospinal fluid layer," *Appl. Opt.* **42**, 2906–2914 (2003).
13. P. van der Zee and D. T. Delpy, "Simulation of the point spread function for light in tissue by a Monte Carlo technique," *Adv. Exp. Med. Biol.* **251**, 179–191 (1987).
14. M. Hiraoka, M. Firbank, M. Essenpreis, M. Cope, S. R. Arridge, P. van der Zee, and D. T. Delpy, "A Monte Carlo investigation of optical pathlength in inhomogeneous tissue and its application to near-infrared spectroscopy," *Phys. Med. Biol.* **38**, 1859–1876 (1993).
15. H. Koizumi, T. Yamamoto, A. Maki, Y. Yamasita, H. Sato, H. Kawaguchi, and N. Ichikawa, "Optical topography: practical problems and new applications," *Appl. Opt.* **42**, 3054–3062 (2003).